PARADe: a low-cost open-source device for photosynthetically active radiation (PAR) measurements

Arnaud Coffin, Bonnefoy-Claudet Clément, Morgane Chassaigne, Arthur Jansen, Christelle Gée

Version of Record: https://www.sciencedirect.com/science/article/pii/S2772375521000186
Manuscript_99f5a7fb8be031cd555b93d3c08a7867

PARADe: a low-cost open-source device for photosynthetically active radiation (PAR) measurements.

Arnaud Coffin [1,*], Clément Bonnefoy-Claudet [2], Morgane Chassaigne [2], Arthur Jansen [2] and Christelle Gée [1, a]

[1] Agroécologie, AgroSup Dijon, INRAE, Univ. Bourgogne, Univ. Bourgogne Franche-Comté, F-21000 Dijon, France;
[2] AgroSup Dijon, 26 boulevard Docteur Petitjean, 21000 Dijon, F-21000 Dijon, France;
[a] ORCID: https://orcid.org/0000-0001-9744-5433;
*Correspondence: christelle.gee@agrosupdijon.fr;

Abstract: In agriculture, proximal in-field information is crucial for a precise management of crop growth. A low-cost, miniaturized and innovative device, named PARADe (PAR Acquisition Device), is designed for in-field photosynthetically active radiation (PAR) acquisition. It combines an affordable PAR line quantum sensor (PAR/LE, SOLEM) and an open source development platform (microcontroller) based on Arduino Integrated Development Environment. The quality of the measurement of the PARADe acquisition chain has been validated. The calibration is done by comparison (R^2=0.99) with a robust acquisition chain composed of a certified PAR sensor (PQS1, Kipp & Zonen) and a data-logger (CR1000 Campbell Scientific). The accuracy of PARADe measurements is evaluated through three indicators, relative error, RMSE and normalized RMSE. They demonstrate that the PARADe system has certain operating limitations especially for low solar angles (sunset and sunrise) due to the choice of a line quantum sensor. This does not affect the accuracy and reliability of the results, but indicates that the PARADe device is specifically adapted to collect daily cumulative PAR values.

Keywords: PAR sensor; calibration; open source; ESP32 card; data logging; Wi-Fi

1. Introduction

In agriculture, to manage and control the crop growth, a fine monitoring of plant biophysical variables such as biomass and chlorophyll is required. These variables are highly dependent on the local environment of the plant and therefore on the available nutrients but also on sunlight which is a key parameter required for photosynthesis process for green plants [1, 2]. Photosynthesis is the bioenergetic process that allows plants to synthesize their organic compounds from incident solar energy interception. The part of this incident solar energy that drives photosynthesis in plants is defined as photosynthetically active radiation (PAR). It concerns the visible light waves range from 400nm to 700nm. The amount of PAR is usually expressed as Photosynthetic Photon Flux Density (PPFD, $\mu mol.m^{-2}.s^{-1}$). Although this parameter is crucial as input data for many ecophysiological models [3, 4, 5], it is often not measured in weather stations. Indeed, for green foliage under non-stressed conditions, it is approximated as a constant value (conversion energy) of the measured global solar radiation (Rg per unit area and expressed in $MJ.m^{-2}.day^{-1}$). Based on summer data in a comprehensive study at 36.6°N latitude (Texas, USA), 48% is taken as a representative fraction of total solar energy that is in the 400–700nm waveband [6, 7]. The temporal variability of this radiation is very important and depends largely on meteorological conditions, which therefore requires a high adaptability of plants [8, 9]. Thus, very precise measurements of this radiation require the sensors to be as close as possible to the cultivated plot. Commercial solutions are proposed but they are very expensive due to the possibility of accommodating several certified PAR sensors at the same time. The main drawback of these systems is that information is encapsulated preventing any modifications of the algorithms. An alternative to these solutions is the use of low-cost and open source connected systems. In [10], Barnard et al. presented a device, called PARduino, combining open source technologies with a proprietary solution concerning the acquisition chain. This hybrid device,

presented as a first foray into the technology world, was a first cost-effective alternative to commercial data-loggers.

The objective of the present study was to design and evaluate the performance of a low-cost open-source device, named PARADe, to automatically measure the in-field photosynthetically active radiation. It combines a non-certified PAR radiation sensor (SOLEM PAR/LE, SOLEMS, Orsay, France [11]) with an acquisition chain containing an electric signal amplifier. First, the design and implement of PARADe are described. Then a calibration of the entire device (PAR sensor and acquisition chain) was provided. The results are presented and discussed in terms of the limits of functioning and of influence of the solar altitude angle. The results of both low-cost devices, PARADe and PARduino were compared and their performances are discussed.

2. Materials and Methods

2.1. PARADe design and presentation

PARADe was designed for logging PAR measurements, in an autonomous way, using open source technology and low-cost elements (Table 1). This device had to meet several criteria: it had to be light (under 15kg) and compact; it also had to be resistant to water and dust while being self-sufficient in energy. All components of the device had to be easily assembled. Finally, the data had to be controlled remotely by a Wi-Fi connection. All components and their price are presented in table 1.

Table 1
List and cost of components (indicative unit price in 2019).

Component	Price (€)
Sensor SOLEMS PAR/LE	256.32
Round tube (1.1 m; diameter 40 mm)	10.90
Legrand junction box 32x24x12 cm	77.16
Base : square tube (1.8m / 40x40mm)	24.00
Rigid PVC (bottom of box and sensor support) 32x24 + 2 * 50x10	23.80
Solar panel support	15.90
Solar panel (10W) + charge controller	64.99
12V 3,2 Ah battery	19.99
ESP32 Wi-Fi microcontroller	11.86
Step-Down Converter 3,3V	16.28
Real Time Clock DS1307	7.81
Step-Down Converter 5V	13.50
Connection plate Proto Shield ARDUINO	4.80
Rail-to-rail amplifier AD 623	6.35
4700 Ω resistor X1	0.14
2200 Ω resistor X1	0.14
1000 Ω resistor X1	0.14
220 Ω resistor X1	0.13
10000 Ω resistor X1	0.14
Push button switch	0.59
LED	0.43
Wires	1.85

Cable gland X3		3.67
ARDUINO alimentation cable for 9V battery		3.00
CR1225 battery		2.90
2 way PCB terminal block x3		2.40
	TOTAL	**569.19**

To get an autonomous device that operates many weeks without interruptions, a solar panel, charge controller and a 12V battery were fixed to the frame device. A 10W solar panel allowed having a comfortable safety margin without alimentation cuts especially in winter when the nights are longs and the days are fully clouded.

The design of the experimental device was an important part of the project (Fig. 1A). It included a non-certified PAR line quantum sensor (PAR/LE). The electronic circuit is composed of a ESP32 card and its shields; the electronic amplification circuit and the electric components (charge controller, battery) were placed in a waterproof junction box . This box was fixed on a mast and, at the opposite, was fixed the solar panel to balance the weights. The PAR sensor was put at the top of the mast. It was fixed on an adjustable plate with a bull's eye level to adjust horizontality. The base of the mast consisted of a removing metal cross with holes to stake the experimental device with pins in soil.

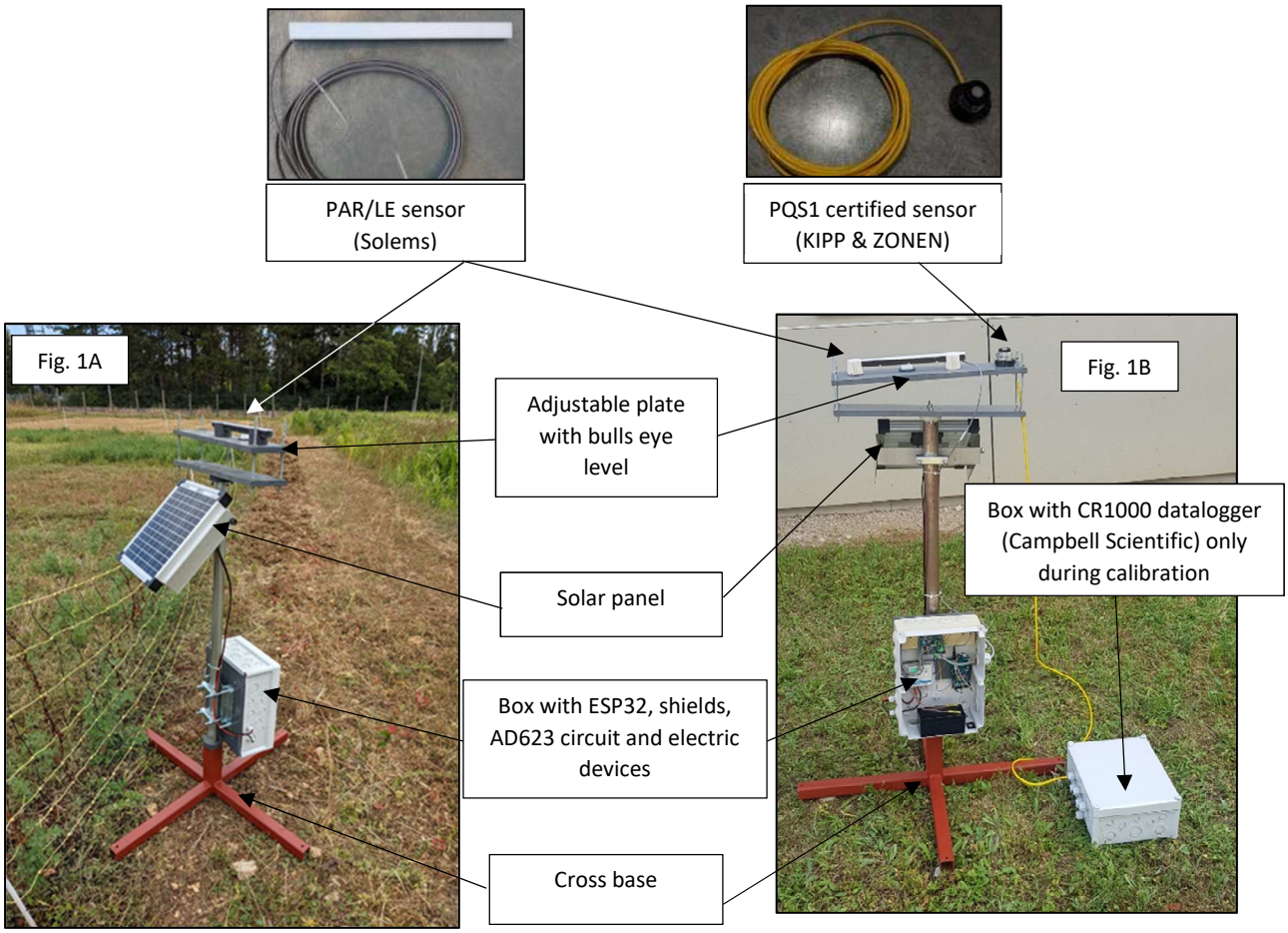

Fig. 1A) PARADe device (PAR/LE sensor + acquisition chain) placed in the agronomic field of AgroSup Dijon (47° 18' 34.443" N ; 5° 3' 57.410" E). **Fig. 1B)** PARADe in presence of the certified PQS1 sensor and the CR1000 data-logger during the calibration phase.

2.2. Photosynthetically active radiation sensor

The PAR/LE sensor from the SOLEMS brand has been selected. It measures Photosynthetically Active Radiation (PAR) integrated by an amorphous silicon photovoltaic cell installed in a plexiglass case and embedded in the polyurethane over its 0.3m line (Fig.1A and Fig.1B). This is a line quantum sensor commonly used for research purposes to measure PAR light above and below the plant canopy where light field is non-uniform [12]. This sensor was delivered without calibration certificate. SOLEMS makes a pre-calibration by sensor batchs, which is not sufficient to record exactly the PAR values. PAR is expressed in unit of Photosynthetic Flux Density ($\mu mol.m^{-2}.s^{-1}$) since photosynthesis is a quantum process [1]. As the PAR is related to the global solar radiation, measurements are very dependent on the solar elevation angle defined as the angle between the sun's rays and the horizontal plane. This angle varies throughout the day and its calculation depends on the latitude of a position and the time of a day in a year. The purchase of unqualified equipment for reliable data requires a calibration phase based on the use of a certified PAR quantum sensor (See section 2.5).

2.3. Signal chain with amplifier

It should be noted that the output voltage (OV) of the PAR sensor is too low (under 100 mV) to be directly readable by an ESP32 card. Thus, an amplification circuit using a rail-to-rail amplifier was set up. The low power consumption ESP32 card, while providing Wi-Fi and Bluetooth connectivity, was also used as a data-logger. The choice of this low power card was partly linked to the low computing power of the card, which was sufficient for our study: few data and few calculations. This card is an easy-to-use solution without operating system to install. No peripherals, such as a monitor or a mouse, are required, as is the case with more powerful cards. As with Raspberry, the ESP32 programming language is based on that of Arduino. The open-source Arduino software (IDE) was used. It is relatively easy for someone with basic programming background and there are many tutorials and a large community of users. This card was used to record (Memory 4MB) an analogic signal as the output voltage of PAR sensor to convert it into digital signal. The card can read the analogic voltage values between 0 and 2.56V or 0 and 3.3V or 0 and 5.5V. This reading is done with a 10 bits resolution whether 1024 values ranging from 0 to 1023. To have the finest resolution in term of digital signal, an output voltage between 0 and 2.56V was chosen. The higher the output voltage from the sensor, the higher the analog reading. Additional components had been integrated to the ESP32 card, such as a Real Time Clock (RTC DS 1307) to record the time of the acquired data. To achieve voltage amplification without additional cost, a low cost voltage amplification chain was developed (Fig. 2).

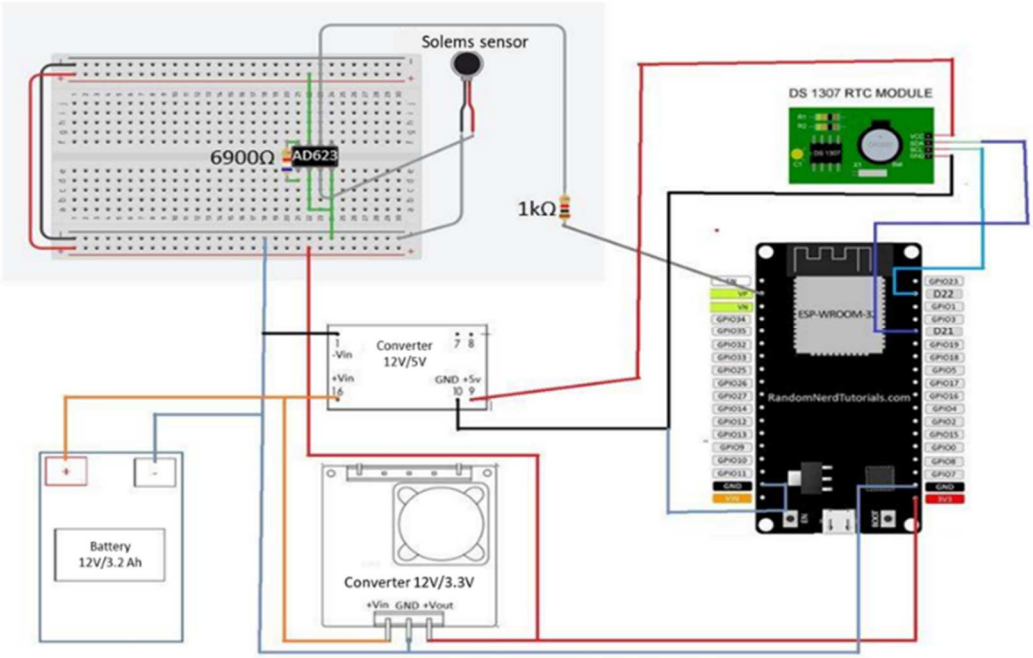

Fig.2. The circuit design of PARADe including an ESP32 card and a Real Time Clockn an amplifier (AD623) and others electronic components and voltage converters.

The amplifier used is the Analog Devices Inc. AD623 Instrumentation Amplifier, which can be alimented by a supply voltage from 2.7 to 12V. It is a rail-to-rail instrumentation amplifier with an input voltage ranging from 0 to 150 mV and it can deliver a linear output voltage whose gain is between 1 and 1000. The value of the gain can be selected according to the value of an external resistor deduced from the following equation.

$$Gain\ AD\ 623 = \frac{V_o'}{V_i'} = \left(\frac{100}{R_G}\right) + 1 \quad (1)$$

With R_G the external resistor ($k\Omega$).

Several empirical tests with different resistance values were made in order to obtain output voltage (Vo) values readable by the ESP32 card. This also made it possible to know precisely the gain of the PARADe amplification chain. To amplify the input voltage (Vi) of the PAR/LE sensor, the resistor value has been chosen to 6900 Ω. The response curve AD623, whose equation is described below, indicates a strong amplification with a positive offset.

$$V_0 = 23.75 \times V_i + 551.3 \quad (mV) \qquad \text{with} \quad R^2=1 \quad (2)$$

2.4. Program and recording process

Fig. 3 presents the data-recording program specifying the different steps. The ESP32 program is detailed in the Appendix A. Every five seconds, the ESP32 card records the output voltage in its intern memory and every 60 values (five minutes) it calculated the average voltage and recorded it in its external memory. At the same time, the ESP32 card records real time clock values and PAR values deduced from the sensor calibration equation. To reduce variabilities resulting from electronic noise and sunlight conditions, data average was performed every five minutes as recommended in the work of Thiebeau and Herre [13], the record of the data average has been done every five minutes. Appendix B describes the webpage written in html language for viewing and downloading the data. A java script has been inserted in the html program allowing to delete or download the data and to stop and re-start the program. While connected to the card's Wi-Fi, you can access the web page by running a web browser and using a local IP address (i.e. 192.168.1.1). The date, time and PAR values are then recorded in CSV format readable by spreadsheet software.

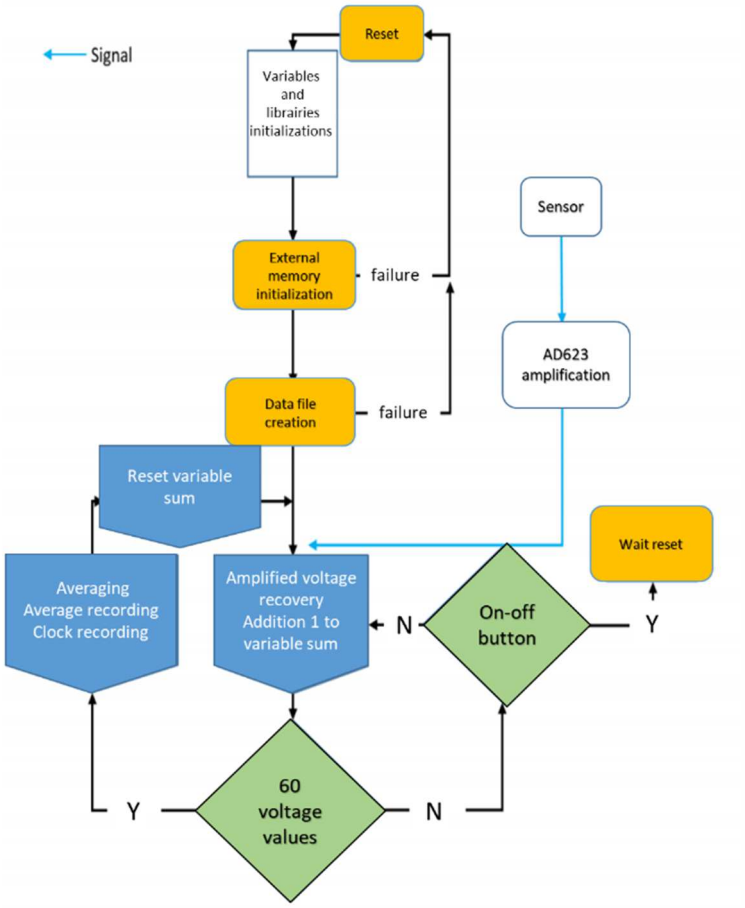

Fig. 3. Flowchart of the PARADe.

2.5. Method of calibration

The calibration phase allowed determining the calibration curve of the entire PARADe device. It represents the evolution of the output voltage of the PARADe acquisition chain as a function of the PAR signal. The calibration phase requires the use of a certified PAR quantum sensor. The PSQ1 (Kipp and Zonen, Netherlands) sensor was chosen and positioned close to the PAR line quantum sensor (Fig. 1B). The calibration of the PQS1 sensor is given by the linear equation between the sensor output voltage (OV, mV) and the irradiance (PAR, $\mu mol.m^{-2}.s^{-1}$). This equation is specific to each sensor and in our case, the equation provided by Kipp and Zonen for this sensor is:

$$OV = 4.7*10^{-3} \times PAR \quad (3)$$

The PSQ1 sensor is connected to a Campbell Scientific Instrument data-logger (model CR1000) that monitored and stored the data. This constitutes the reference device. The data-logger operation was the same as for the ESP32 card: every five minutes, the average of 60 measurements was recorded in a data file. Moreover, the PQS1 sensor voltage was transformed according to Eq. 3). The voltage values from the non-certified PAR/LE sensor (SOLEMS) were recorded by the PARADe acquisition chain (ESP32 board ans amplifier) and were plotted according to the PAR radiation values measured by the certified sensor, PSQ1. For this calibration, as well as for the other tests that were done, data with a PAR value less than 100 $\mu mol.m^{-2}.s^{-1}$ were deleted. Indeed, it has been demonstrated that these values, generally have a high variability [10], are not significant and represent only a small proportion of the daily PAR measurement.

2.6. Accuracy of measurements

To verify the accuracy of the measurement acquired by this PARADe, a relative error (RE) profile was carried out. This profile is a graph representing the evolution of the RE values as a function of PAR values deduced from the reference device. For each measurement, RE was calculated as the difference between values measured by PARADe ($PAR_{calculated}$) and values issued from the calibrated sensor (PAR_{true}) over the PAR_{true}. The formula for the percent error (RE, %) is given below:

$$\text{Percent Error (RE, \%)} = \left(\frac{PAR_{calculated} - PAR_{true}}{PAR_{true}}\right) * 100 \quad (4)$$

From this graph, it is possible to determine the reliability of PARADe measurements and its limits of functioning according to the range of PAR values. Moreover, to evaluate the performance of PARADe, the PAR values ($PAR_{calculated}$) were analyzed to PAR_{true} values using two other statistical estimators, the Root Means Square Error (RMSE, $\mu mol.m^{-2}.s^{-1}$) and the normalized Root Means Square Error (nRMSE, %). Considering n as the total number of measurements, they are defined as:

$$\text{RMSE } (\mu mol.m^{-2}.s^{-1}) = \left[\frac{1}{n}\sum_{i=1}^{n}(PAR_{true_i} - PAR_{calculated_i})^2\right]^{0.5} \quad (5)$$

$$\text{nRMSE } (\%) = RMSE \ / < PAR_{calculated} > \quad (6)$$

2.7. Technical characteristics of PARduino device

In this section, another low-cost device, PARduino [10], is presented. The aim is to compare the PARADe results to a similar tool. The PARduino has been developed for recording PAR radiation values on an Arduino card using a LI-COR Quantum (PAR) circular sensor (Model LI-190SA, LI-COR, Inc., Lincoln, NE, USA) with a commercial amplifier (EME Systems 2007) [14]. The table 2 summarizes the characteristics of both devices, PARduino and PARADe. The main difference between both devices concerns the signal amplification that is an open-source circuit for PARADe.

Table 2
Comparison of characteristics between PARduino and PARADe.

	PARduino	PARADe
PAR sensor	LI-190SA (LI-COR, Inc., NE, USA)	PAR/LE (SOLEMS, Orsay, France)
Calibrated sensor	PQS1 (Kipp and Zonen)	PQS1 (Kipp and Zonen)
Amplifier	EME Systems UTA /BNC/190	AD623
Total cost (without frame device)	685 USD (~578€)	427.6 €

3. Results and Discussion

3.1. PARADe Calibration

Fig. 4 presents the calibration curve (black dots) of PARADe. Hundreds of measurements were obtained by performing a continuous acquisition over few days in July 2020, from 2020/07/24 at 4:00 p.m. to 2020/07/27 at 9:11 a.m.. The correlation coefficient is very close to one indicating a very strong correlation between the voltage issued from PARADe and the PAR radiation (PAR_{true}). The

205 signal that seems noisy for some values of PAR probably corresponds to artifacts or other electronic
206 interferences.

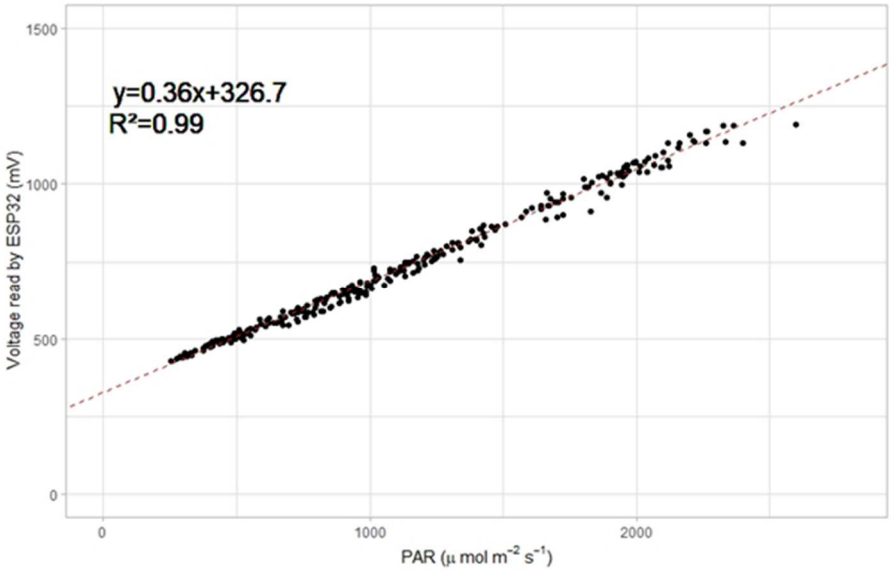

Fig. 4 Calibration curve of the entire PARADe (PAR/LE sensor + acquisition chain) as a function of PAR_{true}. Night-time and non-clear-sky periods were removed from the original dataset.

207 *3.2. Data Validation*

208 First, the performance of the PARADe acquisition chain has be studied and compared to the Campbell
209 Scientific Instrument data-logger (model CR1000). After the PAR/LE sensor output, a bypass has been
210 installed to measure at the same time, the output voltage with both acquisition chains. A strong
211 agreement between both acquisition chains is observed in Fig. 5. However, the signal seems to be
212 slightly noisy suggesting structured fluctuations rather related to electronics but without being able to
213 define the cause.

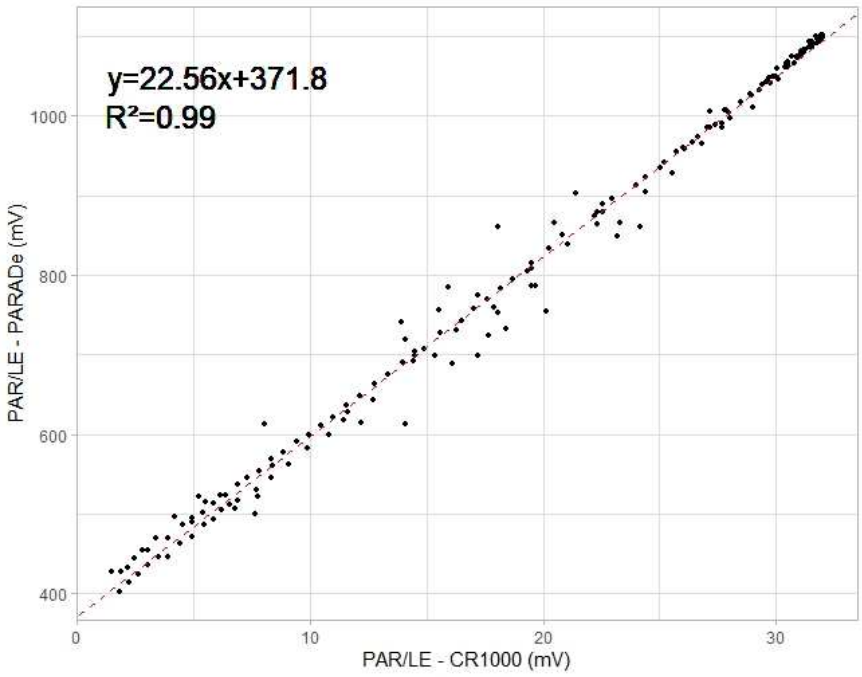

Fig. 5. Voltage measured by PARADe acquisition chain versus the Campbell data-logger.

Then the accuracy of the measurement performed with PARADe was evaluated. The percent error profile (RE, %) in PARADe measurements is presented in Fig. 6 as a function of the PAR_{true}. In addition, for each PAR measurement, the solar elevation angle has been calculated. Graphically, the points have been represented by different colors: the color red corresponds to low solar elevation angle values and the color green is associated with high solar elevation angle values. For intermediate cases, the points are in yellow. The RMSE and nRMSE between $PAR_{calculated}$ and PAR_{true} are calculated. Table 3 summarizes the performance results of PARADe over the entire dataset.

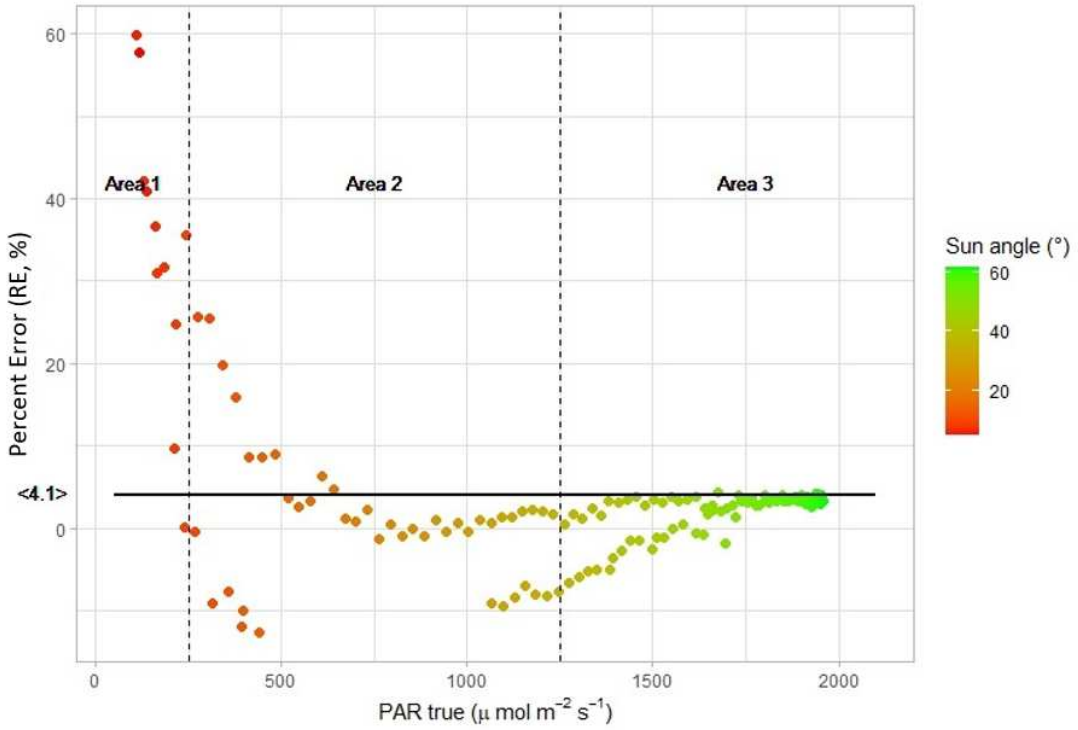

Fig.6. Profile of the percent error (RE, %) as a function of the true PAR values. The black horizontal line indicates the overall average RE for the dataset (mean ER =4.1%). The color legend for the RE values corresponds to the solar elevation angle.

Regarding the shape of the percent error profile, different comments can be made. It reveals that depending on the PAR values, the RE values vary differently. Visually, in this profile three ranges of RE values (high, zero and low values) seems to be distinguished. This would therefore indicate that PARADe operates differently depending on the PAR measurement ranges. Area 1 is represented by a very high value of the average RE when the PAR radiation is low (less than 250 $\mu mol.m^{-2}.s^{-1}$). For this area, the average RE is 33.6 % which indicates a significant overestimation of the $PAR_{calculated}$ with low measurement precision (standard deviation 17.9%). Area 2 was defined for an average RE value close to zero when the PAR values are between 250 and 1250 $\mu mol.m^{-2}.s^{-1}$. The average RE value is 0.8 (± 8.7) % indicating high accuracy of the PAR measurements but with low measurement precision. Finally, for area 3, when the PAR is higher than 1250 $\mu mol.m^{-2}.s^{-1}$, the average RE is 2.1 (± 2.6) % indicating a slight overestimation of the $PAR_{calculated}$. Over the entire range of measured PAR values, the average RE is 4.1% with 11% heterogeneity. However, it can be notice that on Figure 6 most of the points are below the average value of RE, indicating an underestimation of the PAR (Eq. 3). Moreover, all these points seem to be subdivided into different populations whose origin is not clear. Perhaps, is it related to the orientation of the line quantum sensor to the sun or other artifacts (i.e. clouds, brightness)?

Despite the high average RE value observed on the low PAR values (250 µmol.m^{-2}.s^{-1}), it ultimately has little impact on the overall result. Indeed, if PARADe is used to obtain the daily PAR value, deduced from the integration of all the PAR data of a day. Thus, these low PAR values, where the ER is high (Area 1), can be neglected as they represent only a very small proportion of the daily PAR. This reinforces the idea of pursuing the development of such a device, inexpensive for access to accurate and representative daily PAR values.

In addition to the mean and standard deviation of the percent error, the table 3 presents the RMSE and nRMSE for each area and for the entire dataset. Regarding the RMSE values obtained for each zone, they are quite similar and close to the value obtained on the global range of measurements. Looking at the normalized RMSE values, we can see that area 1 has the highest nRMSE. This again confirms that PARADe does not give reliable measurements for this area. However, for the two other areas, the nRMSE values are similar and lower than that of area 1.

Table 3
Values of different estimators (mean of RE, Standard deviation of RE, RMSE and nRMSE) of the PARADe according to the three studied areas and over the entire range of measured PAR values.

PAR (µmol.m^{-2}.s^{-1})	Area 1 [0 – 250]	Area 2 [250 – 1250]	Area 3 [1250 et 2500]	Total [0 – 2500]
Number of measurements	11	45	91	147
mean RE (%)	33.6	0.8	2.1	4.1
sd RE (%)	17.9	8.7	2.6	11
RMSE (µmol.m^{-2}.s^{-1})	56.2	47.8	56.7	54.1
nRMSE (%)	25.0	6.2	3.3	4.1

In an attempt to interpret this overestimation of PAR values in Area 1, we note that the RE values (red dots) are associated with low solar elevation angles (<20°) that correspond to sunrise or sunset. Looking at the Standard ISO 9847 [15], it indicates that, in practice, radiation measurements with the sun altitude angle less than 20° (at sunrise sun and sunset) need to be excluded. The explanation given in the standard is that the response of this type of linear sensors to these radiations is of poor quality and are ultimately inherent to the shape of the sensor [15]. Thus, ours results confirm these comments highlighting the limits of the sensor PAR/LE to detect low solar angle. Finally, PARADe is appropriate for daily PAR measurements because the high variability of the values at sunrise and sunset ultimately have no impact on the daily values (integration of all one-day PAR data). To overcome this problem due to the sensor, one solution proposed is to fix it on an orientable platform to follow the orientation of the sun [16, 17].

3.3. Comparison to PARduino

The Table 4 compares the accuracy of the PARADe device to that of the PARduino. The performances of these two devices were studied over the same range of PAR measurements. Both devices present the same difficulty in measuring low PAR values when the sun is low in the sky. In addition, they present similar results concerning the mean and standard deviation of RE. However, PARduino underestimates PAR with a mean percent error of (-3.49 ± 3.88) % whereas PARADe overestimates them with a mean percent error of (4.1± 11) %. Over the entire range of measured PAR values, PARduino device seems more reliable than PARADe device where the standard deviation is higher for PARADe device. However, for PARADe device, considering only the high values of PAR, for a

measurement range higher 800 µmol.m^{-2}.s^{-1} no percent error value (RE) higher than 10% is observed, unlike the PARduino which has 5 % of its values higher than 10% [10].

Table 4
Performance comparison of the two devices, PARduino and PARADe.

	PARduino	PARADe
Mean percent error (%)	-3.49 (± 3,88)	4.1 (± 11)
Average error compared to a certified measuring chain (µmol.m^{-2}.s^{-1})	-22.00 (± 23,44)	26.1 (±47.1)

4. Conclusion

Compared to other available devices, PARADe is effective for PAR measurements especially for values higher than 250 µmol.m^{-2}.s^{-1}. In addition, the measurement quality of the PARADe acquisition chain has been validated. For this series of measurements, the calibration, carried out by comparison with a robust acquisition chain, was performed only once, but thereafter it is recommended to check it regularly (once a year). However, we must remain cautious about its limits of use because these results indicate a high accuracy with a low precision of data. Therefore, the PARADe system will be rather well geared to collect daily cumulative PAR values. These daily cumulative PAR values can then be used as input parameters for ecophysiological models to develop decision support tools to assist agronomists in monitoring crop production. Subsequently this device could be improved by connecting it to other similar devices or to proximal sensors (temperature, humidity) and by collecting all of this information remotely via a private Low Power Wide Area Networks (Sigfox or LoRaWAN communication protocol for example) dedicated to the deployments of internet of things (IoT). These low-cost devices offer new opportunities in agriculture for smart farming allowing end users (i.e. farmers, technical or engineer staff of institute) less dependent from a brand.

5. Appendices

Appendix A : ESP32 algorithm - Arduino

```
#include <AsyncTCP.h>
#include <Wire.h>
#include "StringArray.h"
#include <SPI.h> // Pour la communication SPI
#include "RTClib.h"
#include <WiFi.h>
#include "ESPAsyncWebServer.h"
#include "SPIFFS.h"
//#include <WebServer.h>
char date[20];
RTC_DS1307 rtc;

int totalgris=0;
int totaljaune=0;
int nombrevaleurs=0;
int controle;
int ledpin=2;
File par;

char* ssid="STATIONPAR2";
char* password="12349876";

IPAddress local_IP(192, 168, 1, 1);
IPAddress gateway(192, 168, 1, 1);
IPAddress subnet(255, 255, 0, 0);
AsyncWebServer server(80);

void setup(){
    nombrevaleurs=0;
  controle=1;
  pinMode(2, OUTPUT);
  WiFi.softAP(ssid,password);
  delay(2000);
  WiFi.softAPConfig(local_IP, gateway, subnet);
  WiFi.persistent(false);
  Serial.begin(115200);
  Serial.print("Adresse IP: ");
  Serial.println(WiFi.softAPIP());
  if(!SPIFFS.begin())
  {
    Serial.println("Erreur SPIFFS...");
    return;
  }

  File root = SPIFFS.open("/");
  File file = root.openNextFile();

  while(file)
  {
    Serial.print("File: ");
    Serial.println(file.name());
    file.close();
    file = root.openNextFile();
  }
 server.on("/", HTTP_GET, [](AsyncWebServerRequest *request)
  {
```

```
    request->send(SPIFFS, "/page.html", "text/html");
  });

  server.on("/w3.css", HTTP_GET, [](AsyncWebServerRequest *request)
  {
    request->send(SPIFFS, "/w3.css", "text/css");
  });

  server.on("/script.js", HTTP_GET, [](AsyncWebServerRequest *request)
  {
    request->send(SPIFFS, "/script.js", "text/javascript");
  });

  server.on("/download", HTTP_GET, [](AsyncWebServerRequest *request)
  {
    controle=0;
    request->send(SPIFFS, "/PAR.csv", "text/csv");
  });

  server.on("/delete",HTTP_GET, [](AsyncWebServerRequest *request){
   SPIFFS.remove("/PAR.csv");
   Serial.println("fichier supprimé (ou pas)");
   request->send(200);
  });
  server.on("/restart",HTTP_GET, [](AsyncWebServerRequest *request){
    ESP.restart();
  });

  server.on("/value", HTTP_GET, [](AsyncWebServerRequest *request)  {

    String enregistrements = String(nombrevaleurs);
    request->send(200, "text/plain", enregistrements);
  });
  server.begin();

  par=SPIFFS.open("/PAR.csv","w");
  if (par.size() == 0) {
      par.println(F("Date;Moyennetensionsolems;moyenne_tension_etalon"));
      par.flush();
  }
  Wire.begin(21,22);
  }

/** Fonction loop() */
void loop() {
totalgris=0;
totaljaune=0;

  for (int mesures=0; mesures < 60; mesures++){
    while (controle==0){

    }
     digitalWrite(ledpin,HIGH);
     int valeurluegrise=analogRead(36);
     int valeurluejaune=analogRead(39);
     totalgris=totalgris+valeurluegrise;
     totaljaune=totaljaune+valeurluejaune;
    delay(3000);
    digitalWrite(ledpin,LOW);
    delay(2000);
    DateTime now = rtc.now();
  sprintf(date,"%04d/%02d/%02d %02d:%02d:%02d", now.year(), now.month(), now.day(), now.hour(), now.minute(), now.second());
  Serial.println(date);
    }
float moyenne_tension_solems=(((float)totalgris/60)*((float)3300/4095));
float moyenne_tension_etalon=(((float)totaljaune/60)*((float)3300/4095));

  DateTime now = rtc.now();
  sprintf(date,"%04d/%02d/%02d %02d:%02d:%02d", now.year(), now.month(), now.day(), now.hour(), now.minute(), now.second());
  Serial.println("fichier crée");
  par.print(date);
  par.print(F("; "));
  par.print(moyenne_tension_solems);
  par.print(F("; "));
  par.println(moyenne_tension_etalon);
  par.flush();
  nombrevaleurs++;
}
```

Appendix B: HTML program of the web page

```html
<!DOCTYPE html>
<html lang="fr">

<head>
    <title>Serveur STATION_PAR_1</title>
    <meta name="viewport" content="width=device-width, initial-scale=1"charset="UTF-8" />
    <link rel="stylesheet" type="text/css" href="w3.css">
    <script type="text/javascript" src="script.js"></script>
</head>

<body class="w3-animate-opacity">

    <div class="w3-card w3-blue w3-padding-small w3-center">
        <h1>STATION PAR 1</h1>
    </div>
    <div class="w3-margin w3-center w3-card w3-padding-24">
        <a href='/download' class="w3-button w3-green w3-xlarge w3-ripple w3-wide" style='width:50%; height:50%;'>Télécharger</a>
    </div>

    <div class="w3-margin w3-center w3-card w3-padding-24">
        <h3 class="w3-padding">Action sur le programme</h3>
        <button onclick="deleteButton()" class="w3-button w3-red w3-xlarge w3-ripple w3-wide" style="width:40%;">Supprimer </button>
        <button onclick="restartButton()" class="w3-button w3-blue w3-xlarge w3-ripple w3-wide" style="width:40%;">Redémarrer </button>
        <br><br>
    </div>

    <div class="w3-margin w3-center w3-card w3-padding-24">
        <h3 class="w3-padding">Nombre d'enregistrements </h3>
        <p class="w3-xxlarge"><span id="value">0</span></p>
    </div>

</body>

</html>
```

Script.js:

```javascript
function deleteButton() {
    var xhttp = new XMLHttpRequest();
    xhttp.open("GET", "delete", true);
    xhttp.send();
}

function restartButton() {
    var xhttp = new XMLHttpRequest();
    xhttp.open("GET", "restart", true);
    xhttp.send();
}

setInterval(function getData()
{
    var xhttp = new XMLHttpRequest();

    xhttp.onreadystatechange = function()
    {

       if(this.readyState == 4 && this.status == 200)
        {
            document.getElementById("value").innerHTML = this.responseText;
        }
    };

    xhttp.open("GET", "value", true);
    xhttp.send();
}, 2000);
```

Declaration of Competing Interest

The authors declare that they have no known competing financial interests or personal relationships that could have appeared to influence the work reported in this paper.

References

[1] S. Pashiardis, S.A. Kalogirou, A. Pelengaris, 2017. Characteristics of Photosynthetic Active Radiation (PAR) Through Statistical Analysis at Larnaca, Cyprus. Biom. biostat. int. j. 2(2), 1009. https://doi.org/10.36876/smjbb.1009

[2] P.J. Sellers, R.E. Dickinson, D.A. Randall, A.K. Betts, F.G. Hall, J.A. Berry, G.J. Collatz, A.S. Denning, H.A. Mooney, C.A. Nobre, N. Sato, C.B. Field, A. Henderson-Sellers, 1997. Modeling the Exchanges of Energy, Water and Cabon Betwwen continents and the Atmosphere. Science, 275, 502-9. https://doi.org/10.1126/science.275.5299.502

[3] N. Brisson, C. Gary, E. Justes, R. Roche, B. Mary, D. Ripoche, D. Zimmer, J. Sierra, P. Bertuzzi, P. Burger, F. Bussière, Y.M. Cabidoche, P. Cellier, P. Debaeke, J.P. Gaudillère, F. Maraux, B. Seguin, H. Sinoquet, 2003. An overview of the crop model STICS. Eur J Agron. 18, 309-332. https://doi.org/10.1016/S1161-0301(02)00110-7

[4] B.A. Keating, P.S. Carberry, G.L. Hammer, M.E. Probert, M.J. Robertson, D. Holzworth, N.I. Huth, J.N.G. Hargreaves, H. Meinke, Z. Hochman, G. McLean, K. Verburg, V. Snow, J.P. Dimes, M. Silburn, E. Wang, S. Brown, K.L. Bristow, S. Asseng, S. Chapman, R.L. McCown, D.M. Freebairn, C.J. Smith, 2003. An overview of APSIM, a model designed for farming systems simulation. Eur J Agron. 18, 267-288. https://doi.org/10.1016/S1161-0301(02)00108-9

[5] M.H. Jeuffroy, and S. Recous, 1999. Azodyn: a simple model simulating the date of nitrogen deficiency for decision support in wheat fertilization. Eur J Agron. 10, 129–144. https://doi.org/10.1016/S1161-0301(98)00059-8

[6] C.M. Britton and J.D. Dodd, 1976. Relationships of photosynthetically active radiation and shortwave irradiance. Agric. Meteorol. 17, 1–7. https://doi.org/10.1016/0002-1571(76)90080-7

[7] J.S. Amthor, 2010. From sunlight to phytomass: on the potential efficiency of converting solar radiation to phyto-energy. New Phytol. 2010 Dec. 188:4, 939-59. https://doi.org/10.1111/j.1469-8137.2010.03505.x

[8]T. Tomson and G. Tamm, 2006. Short-term variability of solar radiation. Solar Energy 80(5), 600-606. https://doi.org/10.1016/j.solener.2005.03.009

[9] J.C. Sager and J. C. McFarlane, 1997. Growth Chamber Handbook. Radiation. North Central Regional Research Publication no 340, Iowa Agriculture and Home Economics Experiment Station Special Report No. 99, 30.

[10] H.R. Barnard, M.C. Findley, J. Csavina, 2014. A Simple and Inexpensive Device for Logging Photosynthetically Active Radiation. Tree Physiol. 34, 640-645. https://doi.org/10.1093/treephys/tpu044

[11] SOLEMS S.A. 2011. « PAR_LE mode d'emploi/ Manual ». https://www.solems.com/wp-content/uploads/PAR_LE_mode_d_emploi_fr.pdf (UK version: https://www.solems.com/wp-content/uploads/PAR_lux_sensors.pdf).

[12] C. Campillo, M.T.I. García, C. Daza, M. H. Prieto, 2010. Study of a non-destructive method for estimating the leaf area index in vegetable crops using digital images. HortScience 45, 1459-1463. https://doi.org/10.21273/HORTSCI.45.10.1459

[13] P. Thiebeau and C. Herre, 2006. Détermination du pas de temps de mesure du rayonnement global, sans effet sur la mesure journalière vis-à-vis du rayonnement global de référence. (Determination of the overall radiation measurement time step, with no effect on the daily measurement with respect to the reference global radiation.) Le cahier des Techniques de l'INRA (INRA's Techniques Book) 59, 31-36.

[14] EME Systems (2007) Universal transconductance amplifier, user manual. Version 2A. EME Systems, Berkeley, CA. Retrieved from: http://www.emesystems.com/UTA/uta_files/UTA_ver2A_120407.pdf

(15 March 2014, date last accessed).

[15] ISO 9847 : 1992, Solar energy. Calibration of Field pyranometers by comparison to a reference pyranometer.

[16] P. Bordenave, 2020. Mise en oeuvre d'un traqueur solaire et de son instrumentation sur un site forestier. (Implementation of a solar tracker and its instrumentation on a forestry site). Le Cahier des Techniques de l'Inra 2020 (INRA's Techniques Book) 100, 1-14.

[17] A.R. Nadia, N.A. Isa, M.K. Desa, 2018. Advances in solar photovoltaic tracking systems: A review. Renew. Sust. Energ. Rev. 82 (2018), 2548-2569. https://doi.org/10.1016/j.rser.2017.09.077